

Title	Microscopic silicon-based lateral high-aspect-ratio structures for thin film conformality analysis
Author(s)	Gao, Feng; Arpiainen, Sanna; Puurunen, Riikka L.
Citation	Journal of Vacuum Science and Technology A: Vacuum, Surfaces and Films. American Vacuum Society. Vol. 33 (2015) No: 1, 010601
Date	2015
URL	http://dx.doi.org/10.1116/1.4903941
Rights	This article may be downloaded for personal use only.

VTT
<http://www.vtt.fi>
P.O. box 1000
FI-02044 VTT
Finland

By using VTT Digital Open Access Repository you are bound by the following Terms & Conditions.

I have read and I understand the following statement:

This document is protected by copyright and other intellectual property rights, and duplication or sale of all or part of any of this document is not permitted, except duplication for research use or educational purposes in electronic or print form. You must obtain permission for any other use. Electronic or print copies may not be offered for sale.

Microscopic silicon-based lateral high-aspect-ratio structures for thin film conformality analysis

Feng Gao, Sanna Arpiainen, and Riikka L. Puurunen

Citation: *Journal of Vacuum Science & Technology A* **33**, 010601 (2015); doi: 10.1116/1.4903941

View online: <http://dx.doi.org/10.1116/1.4903941>

View Table of Contents: <http://scitation.aip.org/content/avs/journal/jvsta/33/1?ver=pdfcov>

Published by the AVS: Science & Technology of Materials, Interfaces, and Processing

Articles you may be interested in

High aspect ratio iridescent three-dimensional metal–insulator–metal capacitors using atomic layer deposition
J. Vac. Sci. Technol. A **33**, 01A103 (2015); 10.1116/1.4891319

Structural analysis of Au/TiO₂ thin films deposited on the glass substrate
Appl. Phys. Lett. **102**, 091603 (2013); 10.1063/1.4794842

Permeation measurements and modeling of highly defective Al₂O₃ thin films grown by atomic layer deposition on polymers
Appl. Phys. Lett. **97**, 221901 (2010); 10.1063/1.3519476

Highly conformal film growth by chemical vapor deposition. II. Conformality enhancement through growth inhibition
J. Vac. Sci. Technol. A **27**, 1244 (2009); 10.1116/1.3207746

Chemical and structural properties of atomic layer deposited La₂O₃ films capped with a thin Al₂O₃ layer
J. Vac. Sci. Technol. A **27**, L1 (2009); 10.1116/1.3079632



Advance your technology or engineering career using the **AVS Career Center**, with **hundreds of exciting jobs** listed each month!

<http://careers.avs.org>



LETTERS

Microscopic silicon-based lateral high-aspect-ratio structures for thin film conformality analysis

Feng Gao, Sanna Arpiainen, and Riikka L. Puurunen^{a)}

VTT Technical Research Centre of Finland, Tietotie 3, 02044 Espoo, Finland

(Received 30 September 2014; accepted 1 December 2014; published 15 December 2014)

Film conformality is one of the major drivers for the interest in atomic layer deposition (ALD) processes. This work presents new silicon-based microscopic lateral high-aspect-ratio (LHAR) test structures for the analysis of the conformality of thin films deposited by ALD and by other chemical vapor deposition means. The microscopic LHAR structures consist of a lateral cavity inside silicon with a roof supported by pillars. The cavity length (e.g., 20–5000 μm) and cavity height (e.g., 200–1000 nm) can be varied, giving aspect ratios of, e.g., 20:1 to 25 000:1. Film conformality can be analyzed with the microscopic LHAR by several means, as demonstrated for the ALD Al_2O_3 and TiO_2 processes from $\text{Me}_3\text{Al}/\text{H}_2\text{O}$ and $\text{TiCl}_4/\text{H}_2\text{O}$. The microscopic LHAR test structures introduced in this work expose a new parameter space for thin film conformality investigations expected to prove useful in the development, tuning and modeling of ALD and other chemical vapor deposition processes. © 2014 American Vacuum Society.

[<http://dx.doi.org/10.1116/1.4903941>]

I. INTRODUCTION

Atomic layer deposition (ALD) is a thin film deposition method based on the use of repeated self-terminating (i.e., saturating and irreversible) chemisorption reactions.^{1–3} It is already used in several industrial applications such as thin film electroluminescent displays, dynamic random-access memories and complementary metal–oxide–semiconductor field effect transistors.^{4,5} As a multitool of nanotechnology, ALD attracts interest in highly different fields of applications from catalysis to coatings for flexible electronics and from textiles to photovoltaics.

One of the key drivers for the interest in ALD is the ability to grow conformal films, which are uniform in thickness on complex-shaped three-dimensional (3D) substrates even when the thickness is a fraction of a nanometer (or even a fraction of a monolayer). Conformality of ALD films is a general assumption and a direct result of the ideal self-terminating ALD chemistry. Nevertheless, even for the most ideal ALD processes, pulsing sequences need to be adjusted from those used for planar substrates, to achieve a uniform coating inside demanding 3D features.^{6,7} Also, many processes developed as ALD in the laboratory scale and tabulated in review articles⁸ may contain secondary reaction paths of irreversible reactant decomposition and undesired side-reactions of the reactants or the gaseous reaction products,⁹ which decrease the film conformality in 3D features and may even prevent the up-scaling of the process to industrial scale.¹⁰

One reason for the fact that most ALD process studies are carried out on planar substrates, without reporting on the film

conformality, may be the lack of test structures, which would be easy to use, simple to analyze, and readily available. When conformality is investigated, it is most often done in vertical trenches etched into the silicon substrates—either with a modest depth-to-width aspect ratio (AR) of roughly, e.g., 5:1 (Ref. 3) or more demanding AR of about 40:1.^{11,12} With macroscopic lateral high-aspect-ratio (LHAR) test structures,^{13,14} accurate thickness profiles along the gap have been recorded with AR up to 200:1. Because of the macroscopic dimensions (gap size on the order of 100 μm), molecular flow inside these LHAR structures is reached only in high vacuum (e.g., 10^{-4} Torr).

In this work, we present a new type of a silicon-based microscopic LHAR test structure for thin film conformality analysis. The limiting dimension of the structure is in the hundreds of nanometers range. This allows the assumption of molecular flow for the typical ALD pressure ranges (one to tens of millibars), as at these pressures the mean free path of molecules on the order of micrometers to tens of micrometers. We demonstrate the use of the microscopic LHAR test structures ALD thin film conformality analysis in diverse ways, from regular microscopy to thickness line scans and electron microscopy. The ALD Al_2O_3 and TiO_2 processes from $\text{Me}_3\text{Al}/\text{TiCl}_4$ and H_2O reactants are used for testing, as these are among the oldest and most studied ALD processes.⁸

II. EXPERIMENT

The LHAR structures, shown schematically in Fig. 1, were fabricated on 150 mm silicon wafers using the standard surface micromachining techniques. First, a thermal oxide layer, defining the gap height of the cavity (200, 500, and 1000 nm), was grown on the polished silicon surface. Next, a

^{a)} Author to whom correspondence should be addressed; electronic mail: riikka.puurunen@vtt.fi

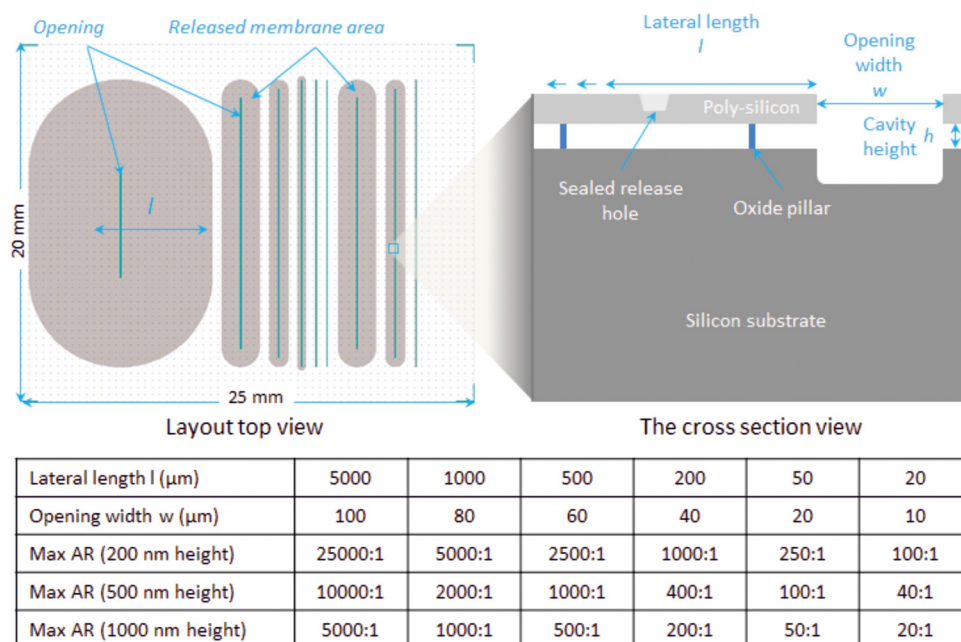


FIG. 1. (Color online) Microscopic LHAR chip layout as top view (top left), side view (top right), and the dimensions used with the resulting AR (bottom).

polycrystalline silicon layer (ca. $1.4 \mu\text{m}$) was deposited on top of the oxide by low-pressure chemical vapor deposition (CVD). Then, the following patented “plug-up” process sequence, which consists of four steps, was carried out.^{15,16}

(1) Release holes were patterned and dry-etched with fluorine-based chemistry through the polysilicon layer and (2) covered by a thin layer of porous polysilicon with pinholes typically in the nanometer range.^{15,16} Then, (3) a vapor phase hydrofluoric (HF) acid etching was carried out to etch the sacrificial oxide through the pinholes in the porous polysilicon layer, thus forming cavities under the polysilicon layer. (4) The pinholes were sealed by a second polysilicon layer deposition (ca. 400 nm) according to the plug-up process.^{15,16} Finally, a port opening was patterned and dry-etched with fluorine-based chemistry through the polysilicon membrane.

Figure 2 shows the SEM cross-section of LHAR structures with 500 nm cavity height. A timed vapor HF etching resulted in unetched oxide pillars, which prevented the

polysilicon membranes from sticking to the substrate silicon after vapor HF etching. The distance between the oxide pillars was $10 \mu\text{m}$.

After the fabrication process, the wafers containing LHAR structures were diced into chips ($20 \times 25 \text{mm}^2$) for coating experiments. The LHAR performance and analysis techniques were demonstrated by ALD films grown in a PICOSUNTM R-150 reactor. The typical pressure range in the reactor was 1–2 mbar. Trimethylaluminum (SAFC Hitech, electronic grade), titanium tetrachloride (SAFC Hitech, electronic grade), and deionized water were used as reactants and N_2 as carrier gas. ALD temperature was varied between 300 and 110°C . Typical pulsing sequence had a 100 ms exposure of Me_3Al or TiCl_4 , a 4 s purge, a 100 ms exposure of H_2O , and again a 4 s purge, and this cycle was repeated until the desired thickness was obtained.

Nikon visible and infrared light microscopes, FilmTek 2000M Reflectometer and Zeiss LEO1560 SEM systems

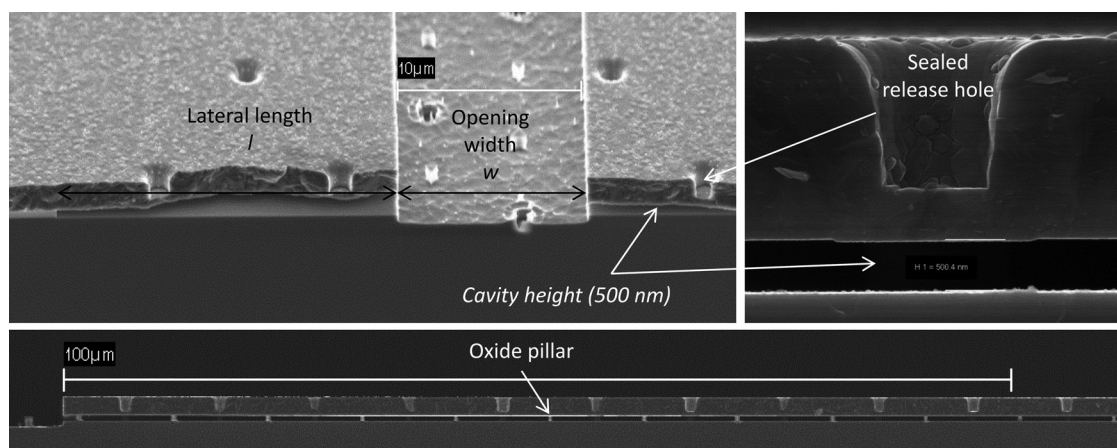


FIG. 2. SEM cross section of a microscopic LHAR structure with a cavity height of 500 nm and (top) AR 40:1 and (bottom) 1000:1.

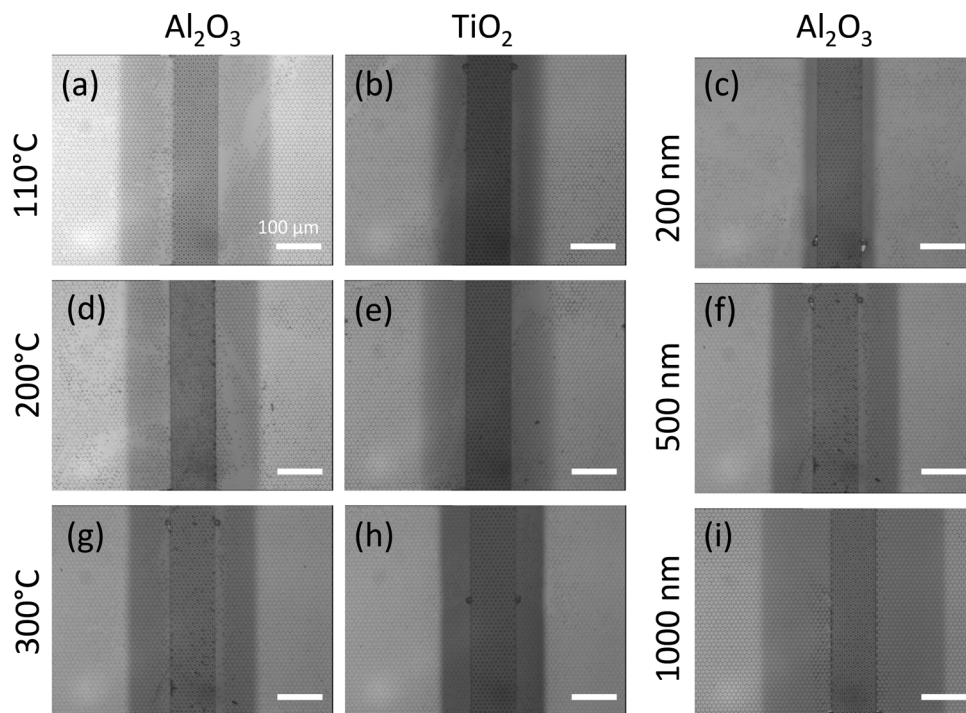


FIG. 3. Top-view infrared microscopy images of ALD Al_2O_3 [(a), (c), (d), (f), (g), and (j)] and TiO_2 films [(b), (e), and (h)] grown at 110°C [(a) and (b)], 200°C [(d) and (e)], and 300°C [(c), (f), (g), (h), and (i)] in LHAR test structures with gap height of 200 nm (c), 500 nm [(a), (b), (d), (e), (f), (g), and (h)], and 1000 nm (i). Target film thickness in all cases was 50 nm. The scale bar in all images is $100\ \mu\text{m}$.

were used to analyze the uncoated and coated microscopic LHAR structures. The reflectometer has a spot size of about $5 \times 5\ \mu\text{m}^2$ with $50\times$ magnification.

III. RESULTS AND DISCUSSION

A. Nondestructive optical top-view analysis

The microscopic LHAR structures consist of a cavity under a thin silicon membrane, with a center opening to allow the penetration of gases for thin film growth. The extent of the film growth under the membrane can be investigated nondestructively through the membrane, for example, by visible-light microscopy as well as by infrared microscopy.

Top-view infrared microscopy images taken of Al_2O_3 and TiO_2 films grown at various temperatures are shown in Fig. 3. Films extend symmetrically in both directions from the center opening. In gaps with 500 nm height, the films extend on the order of $100\ \mu\text{m}$ from the central opening. The dependency of film penetration depth with temperature appears different for Al_2O_3 and TiO_2 : for Al_2O_3 , the penetration depth increases with decreasing ALD temperature, while for TiO_2 the penetration depth first increases and then decreases with decreasing ALD temperature. These trends are related to the changes with temperature in the ALD reaction mechanisms as well as reaction and diffusion kinetics, and exploring them in detail would warrant a dedicated study. The dependency of film penetration depth on the gap height is clear from Figs. 3(c), 3(f), and 3(i): the film extends

to about 25, 90, and $155\ \mu\text{m}$ in the 200, 500, and 1000 nm gaps, respectively.

B. Top-view analysis after membrane removal

An advantage of LHAR test structures is the possibility to remove the top part of the structure and analyze the remaining film on the substrate. In the case of the microscopic LHAR structures, the membrane can be peeled off, for example, by applying adhesive tape.

An example of analyzing the film in the bottom of the cavity after peeling off the membrane is shown in Fig. 4. In

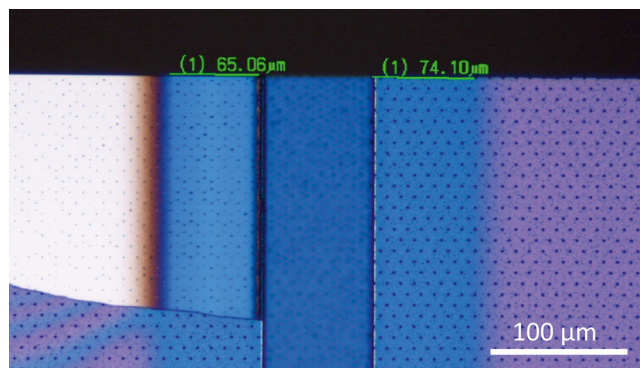


FIG. 4. (Color online) Top-view optical microscopy image of Al_2O_3 grown at 300°C in LHAR with gap height of 500 nm, cleaved to expose the cross section. Target film thickness was 100 nm. The membrane has been peeled off at the left side of the central cavity opening, allowing thickness line scans to be recorded, while at the right side of the central opening the membrane remains intact.

this case, the silicon LHAR chip was cleaved in order to expose the cross section for electron microscopy analysis. On the left, the film under the membrane has been exposed. The penetration of the film inside the cavity can be easily measured by visible-light microscope. In this case, the film extends about $65\ \mu\text{m}$ (AR 130:1) inside the cavity, having the blue interference color typical for a $100\ \text{nm}$ Al_2O_3 film on Si. Beyond this point, the transition of the film interference color through brown at $80\ \mu\text{m}$ (corresponding to $\sim 50\ \text{nm}$ film thickness) to colorless at $90\ \mu\text{m}$ reveals the decrease of film thickness and, eventually, a bare silicon surface. The ending profile of the film is soft, and it takes tens of micrometers for the thickness to decrease to below the detection level.

Perhaps the most powerful means of using the LHAR test structure is to make thickness line scans after the membrane has been peeled off. In the case of the microscopic LHAR test structures, the spot size of needs to be sufficiently small to obtain lateral thickness information.

Examples of thickness line scans made by small-spot-size reflectometer for ALD films on the microscopic LHAR

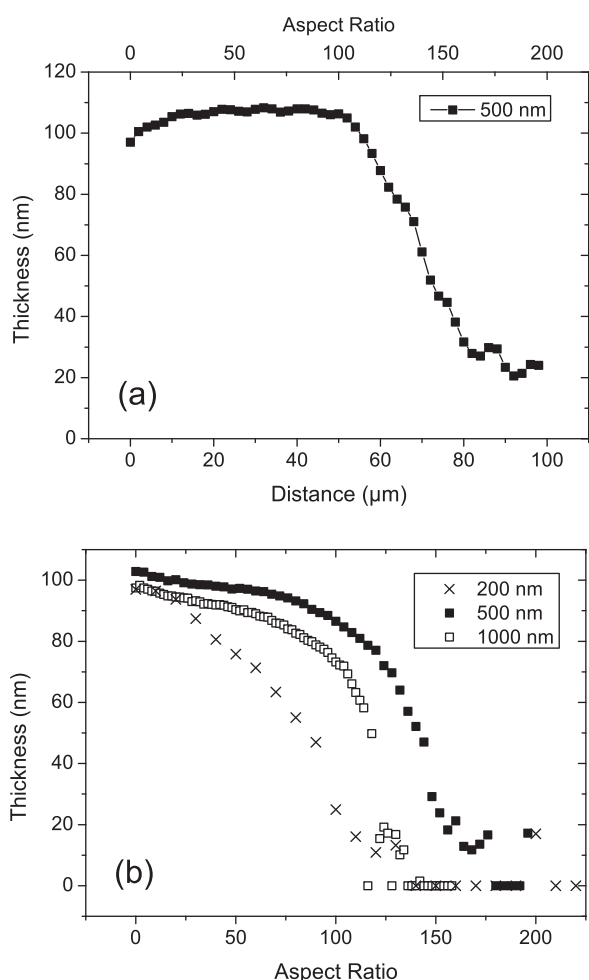


Fig. 5. Examples of reflectometer line scans made after removal of the top membrane of the LHAR structure, for ALD film at the bottom part of the structure. (a) Al_2O_3 processed at 300°C in 1109 ALD cycles, LHAR gap size $500\ \text{nm}$. (b) TiO_2 processed at 110°C in 2000 ALD cycles, LHAR gap size 200, 500, and $1000\ \text{nm}$. The target film thickness was $100\ \text{nm}$.

structures are shown in Fig. 5. Panel (a) shows the variation of ALD Al_2O_3 film thickness inside a cavity with $500\ \text{nm}$ gap size. The film thickness is approximately constant up to a distance of about $52\ \mu\text{m}$ (AR 104:1). Thereafter, the thickness decreases rather linearly. Some waviness is seen in the thickness profile with a period of $10\ \mu\text{m}$, most likely originating from the oxide pillars in the LHAR structure. The reliability of reflectometer measurement decreases for film thicknesses on the order of $10\ \text{nm}$, preventing the accurate measurement of the film ending profile.

Panel (b) shows a comparison of reflectometer line scans for TiO_2 film deposited at 110°C in LHAR structures with cavity height of 200, 500, and $1000\ \text{nm}$. The film thickness profile along the cavity differs significantly from that observed for Al_2O_3 . Instead of being constant along the cavity, the TiO_2 thickness decreases slowly, with a slope that seems to have different values in distinct regimes. In the $500\ \text{nm}$ gap, film thickness decreases to 90% of the original value by AR of 40:1. Around AR of 130:1, the thickness decreases rapidly and is 50% of the original value. Beyond AR 150:1, the thickness is too small to be measured by the reflectometer.

Comparison of the film conformality at different LHAR gap heights allows for the observation of the effect of the physical dimensions on the thin film deposition. The effect of gap height was tested for the TiO_2 process at 110°C . The target film thickness at the entrance was about $100\ \text{nm}$. After the deposition of $100\ \text{nm}$ film, the remaining gap height should be 0, 300, and $800\ \text{nm}$ (original height 200, 500, and $1000\ \text{nm}$, respectively). Therefore, if the AR defined the extent of film growth, it would be expected that the film would reach the furthest in the $1000\ \text{nm}$ -high cavity when compared to the original AR in the uncoated test structure. In contrast to the expectation, the film extended slightly further (as function of the original AR) in the $500\ \text{nm}$ gap than in the $1000\ \text{nm}$ gap [Fig. 5(b)]. This initial result suggests that in addition to aspect ratio, the physical dimensions may also play a role in defining the penetration depth of the coating. For the $200\ \text{nm}$ gap, the narrow opening restricted the film growth as the gap got almost fully closed, and film thickness decreased fastest as function of AR [Fig. 5(b)].

C. Cross-sections by electron microscopy

A traditional way to analyze microscopic HAR structures is to use cross-sectioning and electron microscopy, often in combination with energy-dispersive spectroscopy. The microscopic LHAR test structures are well suited for this type of analysis. The long central opening of the elongated circles makes it easy to cleave the chips with regular laboratory tools such as diamond pen for cross-section analysis.

An example of a cross-section a LHAR structure coated with Al_2O_3 is shown in Fig. 6. The inset show images zoomed in from different locations and reveal that the film extends with the expected thickness of $\sim 100\ \text{nm}$ up to a length of about 120:1. Beyond this, the film thickness starts to decrease. At cavity length of about 200:1, film is no more detected.

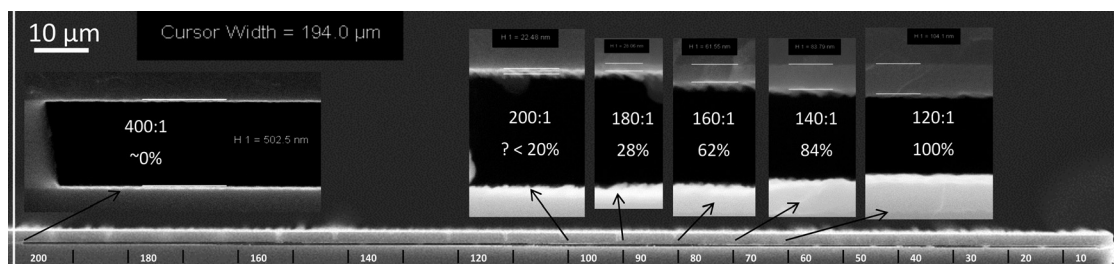


FIG. 6. Cross-sectional SEM image of a microscopic LHAR structure with Al_2O_3 grown at 300°C . The entrance of the cavity is on the right side of the image. The insets show zoomed in views from different locations inside the cavity. The AR was 400:1 and gap height 500 nm.

IV. CONCLUSION

Microscopic silicon-based LHAR test structures were developed for the conformality analysis of thin films. The cavity height was 200, 500, and 1000 nm, giving aspect ratios ranging from 20:1 to 25 000:1. Several means of analysis of the LHAR test structures were demonstrated for characterizing the conformality of ALD Al_2O_3 and TiO_2 films: nondestructive microscopy with visible or infrared light through the top silicon membrane, analysis of the film on the bottom of the cavity by reflectometry after removal of the membrane, and SEM of the cross-section of the LHAR test structure. All techniques gave the same qualitative results of film penetration depth. Film thickness line scans along the cavity furthermore revealed that the film thickness profiles for Al_2O_3 and TiO_2 differed: Al_2O_3 was uniform along the cavity until the point where film termination started, while the TiO_2 thickness decreased slowly but continuously.

The microscopic LHAR test structures introduced in this work expose a parameter space that has earlier been beyond reach in ALD/CVD film conformality investigations. These type of microscopic LHAR test structures can prove useful, for example, for (1) tuning ALD and other thin film processes to reach film coverage in certain aspect ratios (e.g., related to MEMS processing); (2) quickly assess the up-scalability of an ALD process (nonideal reactions such as decomposition and by-product readsorption should manifest themselves as a thickness gradients); (3) providing fundamental information on the kinetics of thin film deposition processes, by comparing the kinetic modeling results with the measurement data obtained for conditions where the assumption of molecular flow is valid.

ACKNOWLEDGMENTS

This work has been made within the Finnish Centre of Excellence on Atomic Layer Deposition by the Academy of

Finland. Discussion with Sergey Gorelick related to the design of the LHAR fabrication process and Christophe Detavernier related to the macroscopic LHAR structures is gratefully acknowledged. Meeri Partanen and Jaana Marles are thanked for clean room processing. The microscopic LHAR test structures were introduced at the Baltic ALD conference in Helsinki, Finland, May 12–13, 2014 and at the 14th International Conference on ALD by AVS, Kyoto, Japan, June 15–18, 2014.

¹R. L. Puurunen, *J. Appl. Phys.* **97**, 121301 (2005).

²S. M. George, *Chem. Rev.* **110**, 111 (2010).

³M. Ritala and M. Leskelä, *Handbook of Thin Film Materials*, edited by H. S. Nalwa (Academic, New York, 2002), Vol. 1, pp. 103–159.

⁴M. Ritala and J. Niinistö, *ECS Trans.* **25**, 641 (2009).

⁵R. L. Puurunen, “A short history of atomic layer deposition: Tuomo sunto-la’s atomic layer epitaxy,” *Chem. Vap. Deposition* (published online).

⁶R. G. Gordon, D. Hausmann, E. Kim, and J. Shepard, *Chem. Vap. Deposition* **9**, 73 (2003).

⁷J. W. Elam, D. Routkevitch, P. P. Mardilovich, and S. M. George, *Chem. Mater.* **15**, 3507 (2003).

⁸V. Miikkulainen, M. Leskelä, M. Ritala, and R. L. Puurunen, *J. Appl. Phys.* **113**, 021301 (2013).

⁹K. E. Elers, T. Blomberg, M. Peussa, B. Aitchison, S. Haukka, and S. Marcus, *Chem. Vap. Deposition* **12**, 13 (2006).

¹⁰A. Yanguas-Gil and J. W. Elam, *Theor. Chem. Acc.* **133**, 1465 (2014).

¹¹I. Jögi, M. Pars, J. Aarik, A. Aidla, M. Laan, J. Sundqvist, L. Oberbeck, J. Heitmann, and K. Kukli, *Thin Solid Films* **516**, 4855 (2008).

¹²M. Kariniemi, J. Niinistö, M. Vehkamäki, M. Kemell, M. Ritala, M. Leskelä, and M. Putkonen, *J. Vac. Sci. Technol., A* **30**, 01A115 (2012).

¹³J. Dendooven, D. Deduytsche, J. Musschoot, R. L. Vanmeirhaeghe, and C. Detavernier, *J. Electrochem. Soc.* **156**, P63 (2009).

¹⁴J. Dendooven, D. Deduytsche, J. Musschoot, R. L. Vanmeirhaeghe, and C. Detavernier, *J. Electrochem. Soc.* **157**, G111 (2010).

¹⁵J. Kiihamäki, J. Dekker, P. Pekko, H. Kattelus, T. Sillanpää, and T. Mattila, *Microsyst. Technol.* **10**, 346 (2004).

¹⁶J. Kiihamäki, U.S. patent 6,930,366 B2 (1 October 2001).